The Astrophysical Journal, 899:140 (13pp), 2020 August 20 https://doi.org/10.3847/1538-4357/ab6f69

A *Gaia*-based Catalog of Candidate Stripped Nuclei and Luminous Globular Clusters in the Halo of Centaurus A

Karina T. Voggel[1,2], Anil C. Seth[1], David J. Sand[3], Allison Hughes[3], Jay Strader[4], Denija Crnojevic[5], and Nelson Caldwell[6]

[1] University of Utah, James Fletcher Building, 115 1400 E, Salt Lake City, UT 84112, USA; karina.voggel@astro.unistra.fr
[2] Universite de Strasbourg, CNRS, Observatoire astronomique de Strasbourg, UMR 7550, F-67000 Strasbourg, France
[3] Department of Astronomy/Steward Observatory, 933 North Cherry Avenue, Rm. N204, Tucson, AZ 85721-0065, USA
[4] Center for Data Intensive and Time Domain Astronomy, Department of Physics and Astronomy, Michigan State University, East Lansing, MI 48824, USA
[5] University of Tampa, 401 West Kennedy Boulevard, Tampa, FL 33606, USA
[6] Harvard-Smithsonian Center for Astrophysics, Cambridge, MA 02138, USA
Received 2019 December 5; revised 2020 January 3; accepted 2020 January 4; published 2020 August 24

Abstract

Tidally stripped galaxy nuclei and luminous globular clusters (GCs) are important tracers of the halos and assembly histories of nearby galaxies, but are difficult to reliably identify with typical ground-based imaging data. In this paper we present a new method to find these massive star clusters using *Gaia* DR2, focusing on the massive elliptical galaxy Centaurus A (Cen A). We show that stripped nuclei and GCs are partially resolved by *Gaia* at the distance of Cen A, showing characteristic astrometric and photometric signatures. We use this selection method to produce a list of 632 new candidate luminous clusters in the halo of Cen A out to a projected radius of 150 kpc. Adding in broadband photometry and visual examination improves the accuracy of our classification. In a spectroscopic pilot program we have confirmed five new luminous clusters, which includes the 7th and 10th most luminous GC in Cen A. Three of the newly discovered GCs are further away from Cen A than all previously known GCs. Several of these are compelling candidates for stripped nuclei. We show that our novel *Gaia* selection method retains at least partial utility out to distances of ∼25 Mpc and hence is a powerful tool for finding and studying star clusters in the sparse outskirts of galaxies in the local universe.

Unified Astronomy Thesaurus concepts: Globular star clusters (656); Elliptical galaxies (456); Ultracompact dwarf galaxies (1734); Galaxy kinematics (602); Star clusters (1567); Galaxy nuclei (609)

Supporting material: machine-readable tables

1. Introduction

In hierarchical structure formation, less massive galaxies are accreted by more massive galaxies, and many of the former are torn apart by the tidal forces they encounter (e.g., Wetzel et al. 2016). This tidal disruption process operates effectively in the low-density outer regions of the accreted galaxies, but the denser central regions survive and live on in their new parent halos (Bekki et al. 2001, 2003; Pfeffer & Baumgardt 2013; Pfeffer et al. 2016). Most galaxies in the stellar mass range $\sim 10^8$–$10^{10} M_\odot$ host dense nuclear star clusters at their centers (e.g., den Brok et al. 2014; Georgiev and Böker 2014; Sánchez-Janssen et al. 2019). The mass of these nuclear clusters ranges from $\sim 10^6$ to $10^8 M_\odot$, correlating with the stellar mass of the galaxies in which they reside (e.g., Georgiev et al. 2016; Sánchez-Janssen et al. 2019). The nuclear star clusters that survive tidal disruption can therefore be used to trace the assembly history of massive galaxies.

There is compelling evidence that, as a class, many of these stripped nuclei have already been identified among the population of ultracompact dwarfs (UCDs). UCDs are loosely defined as star clusters $\gtrsim 10^6 M_\odot$ around galaxies. Most (but not all) UCDs have sizes larger than the typical ∼3 pc half-light radii observed for globular clusters (GCs) with masses $< 10^6\ M_\odot$ (e.g., Norris et al. 2014).

Supermassive black holes were recently found in the centers of five high-mass UCDs (Seth et al. 2014; Ahn et al. 2017, 2018; Afanasiev et al. 2018). The black holes make up 10%–15% of the total mass of these UCDs, a considerably higher fraction than the typical supermassive black hole in a galaxy. Simulations have shown that such massive black holes ($> 10^6 M_\odot$) cannot be made from merged stellar mass black holes and thus the high-mass fraction confirms them as the remnant nuclei of galaxies (Portegies Zwart & McMillan 2002). Other UCDs have shown extended star-formation histories unlike those observed in typical GCs, which is another piece of evidence that they are stripped nuclei (e.g., Norris et al. 2015).

However, while many of the most massive UCDs are likely to be stripped nuclei, there is no clear dividing line between GCs and stripped nuclei in size or mass. The overall fraction of UCDs that are stripped nuclei, and whether that number changes with mass, is very uncertain (Hilker 2006; Brodie et al. 2011; Da Rocha et al. 2011; Norris & Kannappan 2011). A first estimate of the occupation fraction of nuclei among UCDs has been made in Voggel et al. (2019), based on integrated dynamical mass estimates that indicate the presence of a measurable central black hole. That paper shows that the majority of UCDs above $M > 10^7 M_\odot$ are likely stripped nuclei, with this fraction dropping toward lower masses. Among objects with masses $\lesssim 10^6 M_\odot$, only a small fraction have clear signatures of being stripped nuclei, and hence most of these are likely to be GCs.

One fundamental challenge in using UCDs to track a massive galaxy's merger history is identifying a complete sample of stripped nuclei. In nearby galaxies, the stellar halos can cover many degrees on the sky, and both stripped nuclei and GCs are nearly unresolved from ground-based imaging, making their identification difficult. Even with modern, wide

field-of-view spectrographs, it is not currently feasible to obtain spectra of all candidate stripped nuclei. In addition, in some nearby galaxies even radial velocities do not perfectly discriminate between extragalactic objects and foreground Galactic stars.

In this paper we present a method that uses *Gaia*'s exceptional spatial resolution to identify a complete sample of UCDs in Centaurus A (Cen A; NGC 5128). We chose Cen A ($D = 3.8$ Mpc) as the target for this study, as it offers the best place for a feasibly complete search for stripped nuclei in a galaxy that likely hosts many such objects. From previous work, it is clear that Cen A hosts a substantial number of luminous UCDs ($L_V \gtrsim 10^6 L_\odot$), and that at least a subset of these objects show evidence for being stripped nuclei (e.g., Harris et al. 2002; Martini & Ho 2004; Gómez et al. 2006; Rejkuba et al. 2007). Deep ground-based imaging of its stellar halo (Crnojević et al. 2016) has revealed that Cen A has an active accretion history, with a rich system of satellite galaxies and streams, making it a promising location to search for the remnant nuclei of these stripped galaxies. By contrast, the nearest massive galaxies (the Milky Way and M31) lack significant UCD populations. UCDs have been well-studied in cluster environments such as Virgo and Fornax, but the larger distances limit detailed follow-up (e.g., adaptive-optics integral field spectroscopy to confirm supermassive black hole) to only the most massive UCDs.

While these previous pioneering studies have been crucial to establishing an active accretion history and the presence of UCDs in Cen A, no existing study of Cen A offers a complete sample of UCDs, and most known GCs are located within 20 kpc of the galaxy center (Rejkuba et al. 2007; Beasley et al. 2008; Woodley et al. 2010a; Taylor et al. 2016, 2017). The only work going further out is Harris et al. (2012) where they cataloged candidate GCs out to 90 kpc. However, the halo of Cen A extends out to at least 150 kpc. *Gaia* data, combined with existing wide-field photometry (Taylor et al. 2016), enable us to carry out a nearly complete survey for UCDs in the halo of Cen A for the first time.

For the purpose of this work, we use the term UCD to refer to both stripped nuclei and luminous GCs; this term has no connotations of the origin of any particular object. Specifically, we use an apparent magnitude cut of $G < 19$ ($M_G \lesssim -9.7$; see Section 2.2), equivalent to stellar masses $\gtrsim 10^6 M_\odot$. In the Milky Way, the clusters in this mass range include M54, the nucleus of the tidally disrupting Sgr dSph galaxy, and ω Cen, a likely stripped nucleus (e.g., Bekki & Freeman 2003). Our search also comprises UCDs brighter than these objects that are known to exist in Cen A.

We note that while we do not focus on the fainter GCs here, these objects are the focus of an upcoming paper (A. K. Hughes et al. 2020, in preparation). In that paper, we use the deep high-resolution imaging from the Panoramic Imaging Survey of Centaurus and Sculptor (PISCeS) to investigate the population of fainter GCs (Crnojević et al. 2014, 2016, 2019). While we share data sources, our approaches differ; here we emphasize on getting a complete sample of bright objects, while in Hughes et al. we focus on building a large sample of GC candidates at large radii. Many of the sources in our catalog are saturated in the PISCeS imaging, which is why our approach here starts with *Gaia*.

Throughout the paper we apply a distance modulus of $m - M = 27.91$ to Cen A (Harris et al. 2010) and a Milky Way extinction value of $A_g = 0.379$ mag (Schlafly & Finkbeiner 2011).

2. Characterizing Known GCs and Stripped Nuclei in *Gaia* and Ground-based Photometry

Gaia DR2 presents an all-sky astrometric catalog of more than a billion sources (Gaia Collaboration et al. 2018). The current effective spatial resolution of the survey (measured by the ability to resolve closely spaced sources) is $\sim 0\farcs4$ (Evans et al. 2018), though this is expected to improve in future data releases. Since luminous GCs and stripped nuclei have effective radii of $\sim$2–10 pc ($\sim 0\farcs1$–$0\farcs6$ at the distance of Cen A), they appear as marginally extended sources to *Gaia*, which has $0\farcs059$ pixels in the scanning direction. The principle of our method is that the extended nature of these clusters reveals itself in various astrometric measurements, which can be used to select UCDs in a homogeneous manner over the entire Cen A halo.

2.1. Astrometric Excess Noise and the Blue Photometer/Red Photometer Excess Factor

We have identified two DR2 catalog measurements that are useful for selecting extended sources. The first, which is available for nearly all objects, is the Astrometric Excess Noise (AEN). This represents the quality of the astrometric fit and is expected to be zero when all observations fit the model of an individual star perfectly (Lindegren et al. 2018). Extended sources have a higher excess noise compared to a point source.

The second measurement is the Blue Photometer (BP)/Red Photometer (RP) Excess Factor (hereafter abbreviated as $\mathrm{BR_{excess}}$), which is available for most bright (*Gaia* $G < 19$) sources. This is derived from a comparison of the G (broadband) with the Blue Photometer (BP, 3300–6800 Å) and Red Photometer (RP, 6400–10500 Å) magnitudes. While the G magnitude is derived from profile fitting with an effective resolution of $\sim 0\farcs4$, the BP and RP magnitudes are derived directly from the flux within an aperture of 3.5×2.1 arcsec^2 (Evans et al. 2018). $\mathrm{BR_{excess}}$ is defined as the relative flux ratio of the BP + RP fluxes and the G flux. Even for a point source, this value is slightly larger than unity since the BP and RP filters (taken together) have a broader wavelength range than the G filter. For extended sources, the ratio is even larger, since the "extra" light beyond the point source is picked up in the larger BP + RP apertures. However, a high ratio could also indicate contamination from a nearby source (expected in crowded regions), and extended sources could be background galaxies or double stars rather than star clusters.

Most *Gaia* sources in the magnitude range of potential GCs have both excess factors. Of all sources in the vicinity of Cen A, 98.8% of sources between $G = 15$ and 19 mag, and 97.3% of sources in between $G = 19$ and 20 mag have the two excess factors.

To test whether these quantities can effectively select extended sources in *Gaia* DR2, we use a set of confirmed UCDs (massive GCs and candidate stripped nuclei) in Cen A to see whether they have elevated AEN and $\mathrm{BR_{excess}}$ factors. The test sample of velocity-confirmed clusters is taken from various literature sources (Beasley et al. 2008; Woodley et al. 2010a; Taylor et al. 2017). We require that all sources have existing photometric measurements, and select only those objects with $g_0 < 18.8$, corresponding to an apparent limit of $g < 19.1$. We

Table 1
List of Foreground Stars that Were Misclassified as GCs in the Literature

Name Beasley+2008	Name Taylor+2017	R.A.	Decl.	Radial Velocity (km s^{-1})	Vel. Source	g mag (mag)	*Gaia* R.A. Proper Motion (μas yr^{-1})
...	GC0565	201.0275	−42.882944	285.0 ± 29.0	Woodley+2010	17.99	−9.82 ± 0.35
AAT109380	GC0047	201.181583	−43.145333	448.0 ± 31.5	Beasley+2008	18.48	−4.66 ± 0.53
PFF-gc039	GC0133	201.287917	−42.40025	388.2 ± 25.2	Beasley+2008	18.61	−3.58 ± 0.52
PFF-gc046	GC0159	201.311792	−43.686278	526.6 ± 20.4	Beasley+2008	18.61	−4.20 ± 0.65

also exclude sources within 5′ (∼5.5 kpc) of the center of Cen A owing to issues with crowding and extinction. The systematic velocity of Cen A is $v_{\rm helio} = 541$ km s^{-1} and the dispersion of the GCs is $\sigma \sim 150$ km s^{-1} (Peng et al. 2004). Thus, we use a conservative radial velocity cut of $v < 275$ km s^{-1} to remove objects with ambiguous velocities that might instead be Galactic foreground stars. This leaves us with a final set of 61 confirmed UCDs as our test sample.

When we match this sample to *Gaia* DR2, we find that all of the UCDs have a *Gaia* match within 1″ (see also Section 2.2). This indicates that the *Gaia* catalog has a high completeness for Cen A star clusters with $g < 19.1$, at least away from the more crowded central regions of the galaxy.

As a next step, we checked whether any of these literature objects had significant parallaxes or proper motions in *Gaia* (with signal-to-noise ratio (S/N) > 4). This would indicate that these "confirmed" UCDs are actually misclassified foreground stars. We found that 4 of the 61 objects indeed have significant proper motions, indicating that they are Galactic stars. These four objects all had low S/N measurements of their radial velocities in Taylor et al. (2010) and hence it is likely they were misclassified from poor velocity measurements. In Table 1 these misclassified GCs are listed. A complete list of the 57 literature GCs used in this comparison can be found in Table A1 in the Appendix.

The two astrometric quantities (AEN and $\rm BR_{excess}$) are plotted against G for this sample of 61 literature UCDs in Figure 1, using different symbols for the misclassified objects. We compare this sample to that of all *Gaia* sources within 2.°3 of Cen A. The main stellar locus is clearly visible in both panels as a dark blue plume at low values of these excess factors. Notably, the confirmed UCDs all have AEN and $\rm BR_{excess}$ significantly above the stellar locus, showing that these astrometric excess factors can clearly identify the extended nature of these sources.

Guided by these results, we draw boundaries between the extended UCDs and the stellar locus at the 98th percentile of the distributions of AEN and $\rm BR_{excess}$ as a function of magnitude. Cutting sources below the 98th percentile does not remove any literature sources while getting rid of a maximum of stellar contaminants. We then fit the following exponential functions to represent the boundaries:

$$\mathrm{AEN} = 0.12 + 2.66 \times 10^{-6} e^{0.7G} \quad (1)$$

$$\mathrm{BR_{excess}} = 1.39 + 2.18 \times 10^{-7} e^{0.76G}. \quad (2)$$

Figure 1 shows that these boundaries effectively separate confirmed UCDs from stars.

2.2. *How Does the* Gaia *Photometric System Compare to the Literature Photometry?*

Here we compare *Gaia* photometry to that already published in the literature. In particular, Taylor et al. (2017) presents

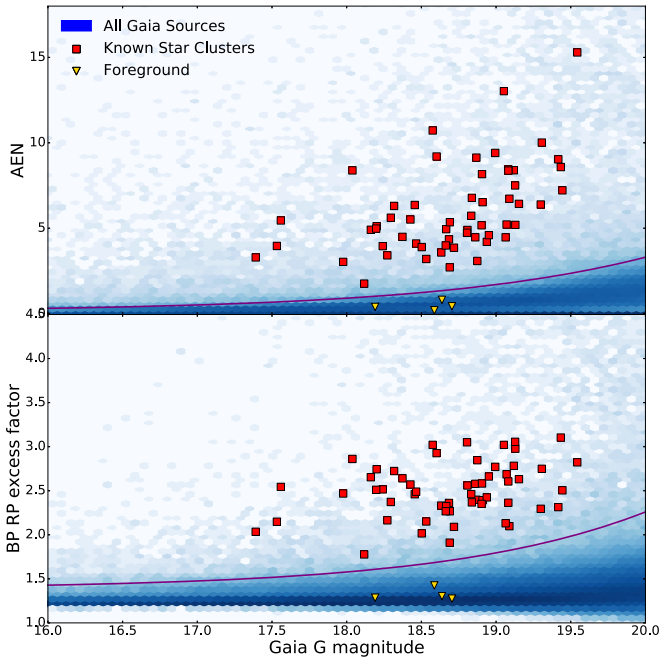

Figure 1. Top: AEN plotted against *Gaia* G magnitude. The blue density plot shows all *Gaia* sources within 2.°3 of Cen A. Red squares are confirmed bright ($g < 19.1$) literature GCs and yellow triangles are misclassified literature GCs (actually foreground stars with high significance proper motions). Bottom: as above, but for $\rm BR_{excess}$ rather than AEN. Both panels show that these astrometric excess factors can effectively select extended objects (included stripped nuclei and GCs) in Cen A.

multiband photometry for a large number of sources around Cen A.[7] In the median, the $G - g$ values for our sample of literature UCDs is 0.19, with an rms scatter of 0.16 mag. This modest scatter shows that we have in fact correctly identified *Gaia* sources for the clusters. Note that the magnitudes quoted here are all extinction corrected unless explicitly mentioned; we assume uniform extinction corrections of $A_V = 0.32$, $A_G = 0.27$, $A_g = 0.37$, and $A_r = 0.26$ (Schlafly & Finkbeiner 2011).

At first consideration, the derived $G - g \sim 0.19$ is surprising, since the $G - g$ color is expected to be ∼−0.4 to −0.7 for the $g - r$ colors of our GCs using the relations from Jordi et al. (2010). To investigate this, we also match stars from Taylor et al. (2017) to *Gaia* that are at the same $u - r$ colors range as the confirmed GCs. We find an offset between the stellar locus and the GCs in $G - g$ of 0.52 mag.

This tells us that the measured G magnitudes of GCs in *Gaia* are half a magnitude fainter than expected since the UCDs are

[7] In the course of this work we discovered that the photometry from Table 2 of Taylor et al. (2017), which states that it is not corrected for foreground extinction, has in fact already had these corrections applied. This photometry is discussed in detail in A. K. Hughes et al. (2020, in preparation).

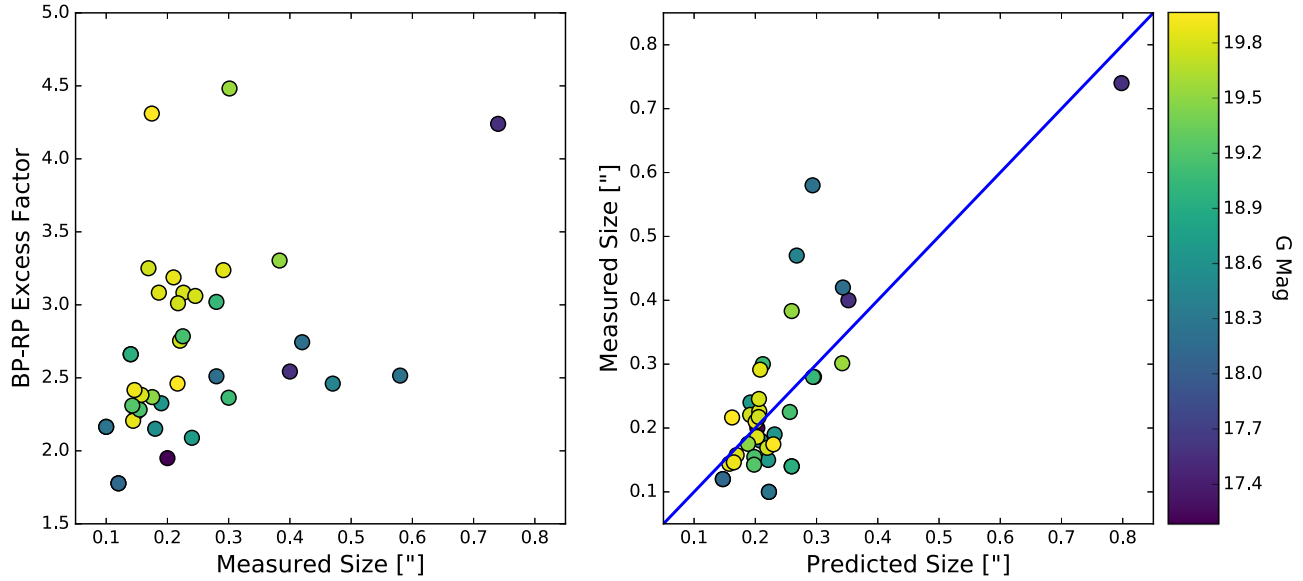

Figure 2. Left: BR_{excess} as a function of the measured sizes of UCDs in Cen A and Virgo. The shading scales with the G magnitude of the source. These quantities are somewhat correlated, but with a large magnitude-dependent scatter. Right: the predicted size from Equation (3) compared to the actual size, showing the improved quality of the correlation once magnitude is considered. This relation has a scatter of about 30%.

resolved and the G mags are measured assuming the profile of a point source. Indeed, this effect is what makes the identification of UCDs with *Gaia* possible.

Correcting our $G - g$ colors by this 0.52 mag offset leads to a range of $G - g$ colors of 0.0 to −0.67 with a mean of −0.32. This erases the bulk of the discrepancy between the observed and expected colors of our sources but the GCs are still an average of 0.2 mag too red compared to the theoretical colors of Jordi et al. (2010).

As another check of the fraction of the flux we are missing from Cen A GCs, we matched the *Gaia* G magnitudes to a sample of Cen A GCs from Peng et al. (2004) which have carefully calibrated V mags. We find $G - V \sim 0.29$, with a dispersion of 0.17 mags. This compares to an expected $G - V$ of ∼−0.25 for typical GC colors (Jordi et al. 2010), suggesting an offset of 0.5–0.6 mags in G, consistent with the 0.52 mag update we found above.

Using the observed $G - V$ color suggests our $G < 19$ limit corresponds to $M_V \lesssim -9.5$ after correcting for extinction. This corresponds to a V band luminosity of $5 \times 10^5\ L_\odot$, which assuming the typical M/L_V of 2 found for GCs (e.g., Voggel et al. 2019) suggests a cluster mass of $10^6\ M_\odot$. Thus, our survey limit corresponds roughly to clusters above $10^6\ M_\odot$.

For the remainder of the paper, whenever we convert the *Gaia* G magnitudes to absolute magnitudes or luminosities, we account for this effect. For instance, the $G < 19$ cut used for our sample corresponds to $M_G \sim -9.7$ after correction for extinction and inclusion of this offset.

2.3. Correlation between Excess Factors and Size

The previous part of this section shows that two *Gaia* astrometric parameters can reliably identify known UCDs in Cen A. Here we test the ability to obtain even more information: since the excess factors quantify how much a given source deviates from a single star model, in principle, larger UCDs should also have larger excess factors.

Only a subset of our sample of confirmed Cen A UCDs have existing reliable size measurements. We find 21 such objects in the literature (Rejkuba et al. 2007; Taylor et al. 2010; Woodley et al. 2010a). To enlarge the sample and test the correlation over a larger magnitude range, we also add 19 UCDs with $G < 20$ and measured sizes from the Virgo Cluster study of Liu et al. (2015).

Figure 2 compares the angular sizes of this composite sample of UCDs with BR_{excess}. These quantities show a correlation; however, the correlation is magnitude dependent, since BR_{excess} also depends on G (see Figure 1).

To account for this, we fit a function that depends on both the magnitude and BR_{excess} to the data:

$$r_h('') = (0.222 - 0.095(G - 18))(BR_{excess} - 2.5) + 0.308(G - 18) - 0.074. \quad (3)$$

This resulting relation is shown in the right panel of Figure 2. While the range of the predictions is modest and the scatter is substantial (rms of 0.″081, which is a fractional scatter of 31%), it still suggests that it is possible to measures the sizes of UCDs with *Gaia* data to an accuracy of ∼30% over the size range ∼0.″1–0.″5. This accuracy is lower than can be achieved using, for example, the *Hubble Space Telescope*, but it is superior to the quality of ground-based sizes in most cases. It would be worthwhile to extend this work to a larger sample over a more uniform range of galaxy distances in the future.

The work above solely concerns BR_{excess}; the AEN measurements have lower S/N, especially for fainter sources, so appear less promising than BR_{excess} for this purpose.

2.4. Broadband Colors of Star Clusters

Another source of information available is *ugriz* broadband photometry from the Survey of Centaurus A's Baryonic Structures (Taylor et al. 2016, 2017) program. They published a catalog of 3200 GC candidates as well as photometry of ∼500,000 point sources in their survey area, extending out to $D_{proj} \approx 150$ kpc from CenA.

It is well-established that the integrated stellar populations of GCs separate in color–color space from contaminants including foreground stars and background galaxies, and that the quality

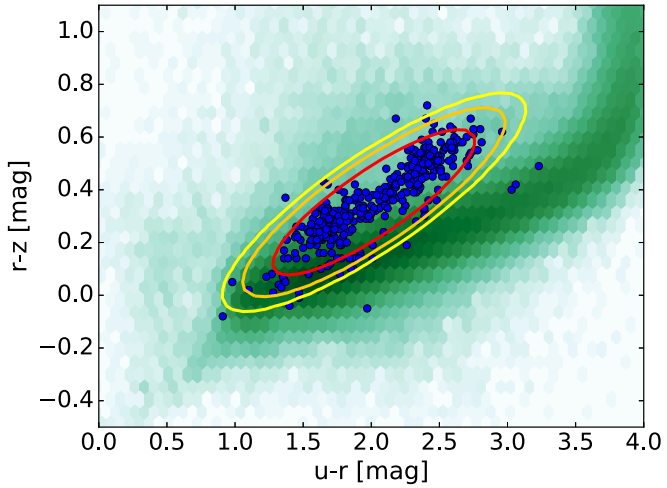

Figure 3. Color–color plot of velocity-confirmed star clusters (blue) and stars (green) around Cen A, with all extinction-corrected photometry taken from Taylor et al. (2017). The red, orange, and yellow ellipses represent the results of mixture modeling that include 85%, 95%, and 97% of all confirmed GCs.

of the separation increases with the width of the baseline (e.g., Strader et al. 2011; Muñoz et al. 2014; Taylor et al. 2017). Here we use the $u - r$ versus $r - z$ color space, where GCs are well-separated at the metal-rich end, although there is some overlap at the metal-poor end.

To do this we first matched the position of velocity-confirmed literature GCs/UCDs (Harris et al. 1992, 2002, 2006; Peng et al. 2004; Woodley et al. 2005, 2007, 2010a, 2010b; Rejkuba et al. 2007; Beasley et al. 2008; Taylor et al. 2010) with the Taylor et al. (2017) photometric catalog of point sources, finding 389 matches. In Figure 3 we show this color–color plot and, as a comparison, Taylor et al. (2017) colors for all *Gaia* sources with $G < 19$ within $2\overset{\circ}{.}3$ of the center of Cen A. The colors use the magnitudes of their Table 2, which are already extinction corrected. As expected, the clusters are well-separated from the dense stellar locus, except at the bluest end of their distribution.

To have a quantitative way to estimate the probability of a photometric source being a UCD based on these color–color data, we use a Gaussian mixture model (Pedregosa et al. 2011) to separate the clusters and stars. The results of this model (see Figure 3) provide a likelihood for each source to be classified as a star cluster.

3. Finding New Luminous GCs and Stripped Nuclei with *Gaia*

Now that we have explored how known GCs and stripped nuclei look in the *Gaia* excess factors and in broadband colors, we can apply this knowledge to the entire *Gaia* catalog around Cen A to find new candidate UCDs.

Our work here is based on the second data release of the *Gaia* mission (Evans et al. 2018; Gaia Collaboration et al. 2018). We download all the *Gaia* DR2 sources within a radius of $2\overset{\circ}{.}3$ of the center of Centaurus A (R.A.: $13^{\rm h}25^{\rm m}27\overset{\rm s}{.}6152$, Decl.: $-43^{\rm d}01^{\rm m}08\overset{\rm s}{.}805$), which is equivalent to a physical radius of 150 kpc, a radius encompassing the imaging data collected by the PISCeS project (Crnojević et al. 2016). This leaves us with an initial catalog of 514,439 *Gaia* sources. From here we make several cuts to narrow down the catalog to the most likely star cluster candidates.

Our selection method follows these steps:

1. We select all *Gaia* sources with $G < 19.0$. This corresponds to UCDs with $M_G \lesssim -9.7$, equivalent roughly to masses $\gtrsim 10^6 M_\odot$ as discussed in Section 2.2.
2. We eliminate foreground stars by cutting sources that have a *Gaia* proper motion in either coordinate or a parallax measurement of $S/N = 4$ or greater, since Cen A UCDs should not have measurable values of these quantities at *Gaia* precision.
3. We next apply a cut in the AEN and BR_{excess}. For this we use the exponential cut-off line to the two excess factors described in Equations (1) and (2) and shown in Figure 1.
4. Our set of 389 confirmed Cen A star clusters has a color range of 0.66–1.6 in BP− RP. Thus, we also apply a broad *Gaia* color cut selecting only sources with $0.6 <$ BP–RP < 1.6 to remove objects from the extreme red and blue end of the distribution where no known GCs are located.

With these selection criteria we get a final list of 632 new candidate UCDs. The distribution of these candidates in AEN and BR_{excess} as a function of magnitude is plotted in Figure 4. We note that making only a cut on AEN would result in 1530 candidates, while making a cut on BR_{excess} only would result in 840 candidates. This suggests both *Gaia* parameters provide useful information for creating a complete sample while minimizing contamination.

3.1. Color Information for the Gaia-selected Cluster Candidates

While we do not yet have the information necessary to definitively determine how many of these candidates are true UCDs, we can investigate our selection criteria function by showing how the density of sources in color–color space changes as we apply our cuts sequentially. The first panel of Figure 5 shows the density distribution of all *Gaia* sources that also have multiband photometry in Table 2 of Taylor et al. (2017). The star cluster sequence is not visible in this panel as it is washed out by the scatter in the overwhelming stellar locus.

The next panel shows the effects of the cuts on G, BP−RP, proper motion, and parallax. This panel is still dominated by a thick stellar locus, but the hint of the UCD sequence is emerging. The third panel finally adds the AEN and $BR_{excesscuts}$, where the sequence of likely Cen A objects is now strong. The final panel is a ratio of the third and first panels, with the UCD sequence boldly visible, showing that our criteria effectively select UCDs, especially among the redder objects where there is less stellar contamination. This figure also shows that *Gaia* data can also significantly improve on color-only selection methods.

3.2. Visual Classification of Candidates

For our next classification stage, we used data from the PISCeS (Crnojević et al. 2014, 2016) taken with the Megacam on *Magellan*, which has imaging data for 346 (about ∼55%) of the 632 UCD candidates; the rest do not fall within the survey footprint. The typical angular sizes of UCDs at the distance of Cen A are $0\overset{''}{.}1$–$0\overset{''}{.}6$ (∼2–11 pc). In good seeing conditions (∼$0\overset{''}{.}5$–$0\overset{''}{.}6$) the outer regions of the UCDs start to resolve into individual red giant branch stars, providing a clear signature of their identity. Such data also work to reject contaminants:

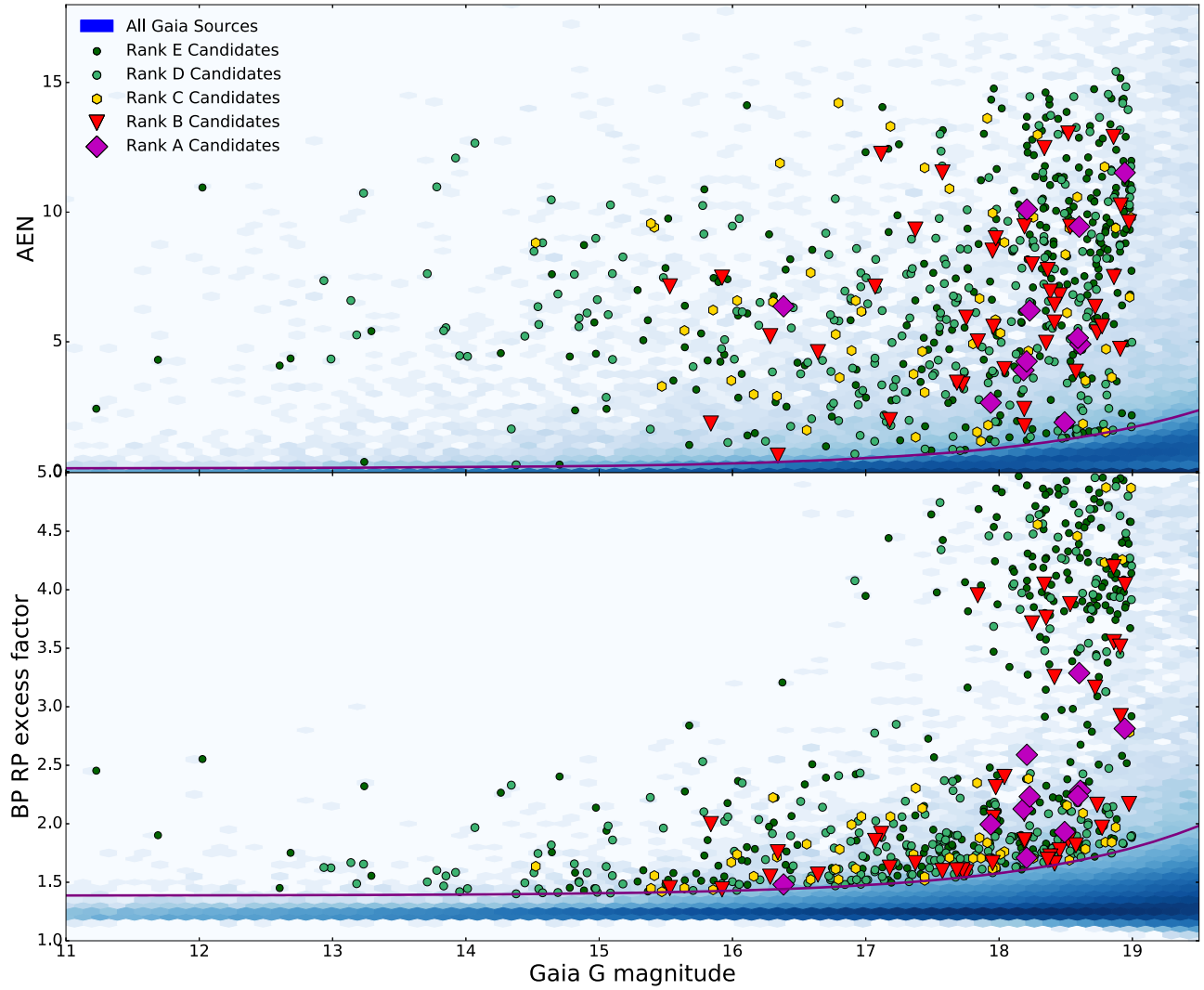

Figure 4. Distribution of the 632 selected *Gaia* sources that pass our UCD selection criteria in the two excess factors against *G* magnitude. The color coding is the final ranking of the candidates (including visual classification), where Rank A candidates (large purple diamonds) are the most likely UCDs and Rank E (small dark green circles) the least likely.

Table 2
List of *Gaia* UCD Candidates

Name	R.A. (deg)	Decl. (deg)	AEN	*Gaia G* (mag)	BP RP Excess	*u*–*r* (mag)	*r*–*z* (mag)	*r* mag (mag)	Votes	C.L.	Rank
KV19-001	198.276663	−42.993805	2.16	18.01	2.02	1.03	−0.16	16.96	nan	0.01	D
KV19-002	198.322490	−43.583197	3.76	16.51	2.19	nan	nan	nan	nan	nan	C
KV19-003	198.334218	−43.114592	7.02	18.73	3.43	nan	nan	nan	nan	nan	C
KV19-004	198.363842	−43.735719	8.24	18.34	3.48	nan	nan	nan	nan	nan	C
KV19-005	198.364438	−43.382436	8.82	14.58	1.41	nan	nan	nan	nan	nan	C

(This table is available in its entirety in machine-readable form.)

background galaxies and close ("double") sets of foreground stars can pass the *Gaia* astrometric cuts but be readily visible by eye.

To formalize our visual inspection of these PISCeS data, we used $1\farcm2 \times 1\farcm2$ cutout images centered on each candidate. After training ourselves on confirmed UCDs, team members carefully examined each image for evidence that the candidate object was resolved into stars in its outskirts or more extended than surrounding point sources. Five team members voted independently on the likelihood that each candidate was a star cluster. These five votes were then averaged to generate a final visual assessment score for each target.

On the basis of a "pilot program" for this visual grading, we decided on four categories, ranging from 1 (most likely to be a UCD) to 4 (least likely). Category 1 UCDs showed clear signs of a resolved stellar halo. Category 2 UCDs showed hints of being extended but without obviously resolved outskirts. Category 3 objects had no evidence for or against them being UCDs; this category often includes objects taken in poor seeing conditions as well. Category 4 objects are obvious non-clusters:

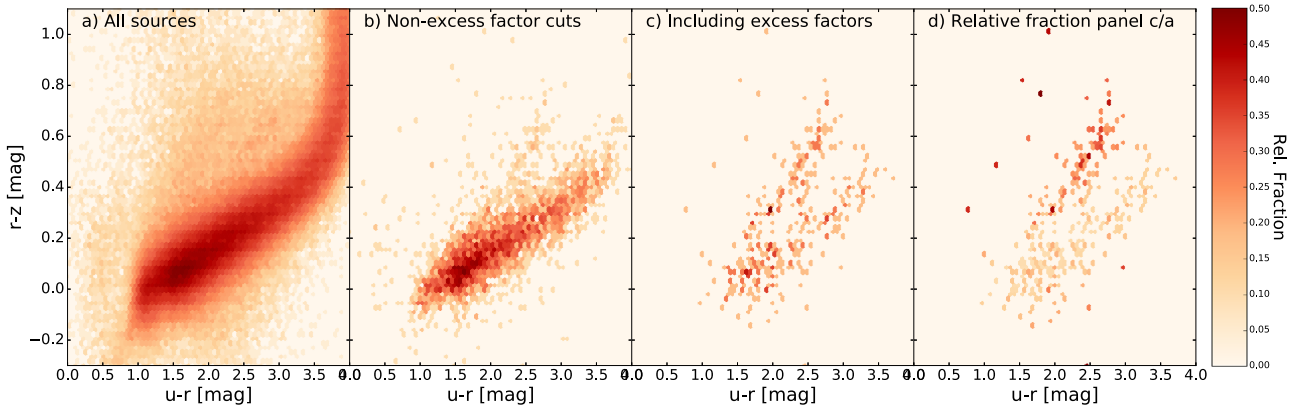

Figure 5. $r - z$ vs. $u - r$ color–color plots, showing the stages of our UCD candidate selection. The left panels shows the density distribution of all point sources from the Taylor et al. (2017) Table 2 that have a *Gaia* match. The second panel has our cuts in G, BP− RP, parallax, and proper motion. The third panel adds cuts in BR_{excess} and AEN. The last panel is the ratio of the third and first panels, i.e., the relative fraction of the third panel with full photometry. This shows that our method does effectively select likely UCD candidates.

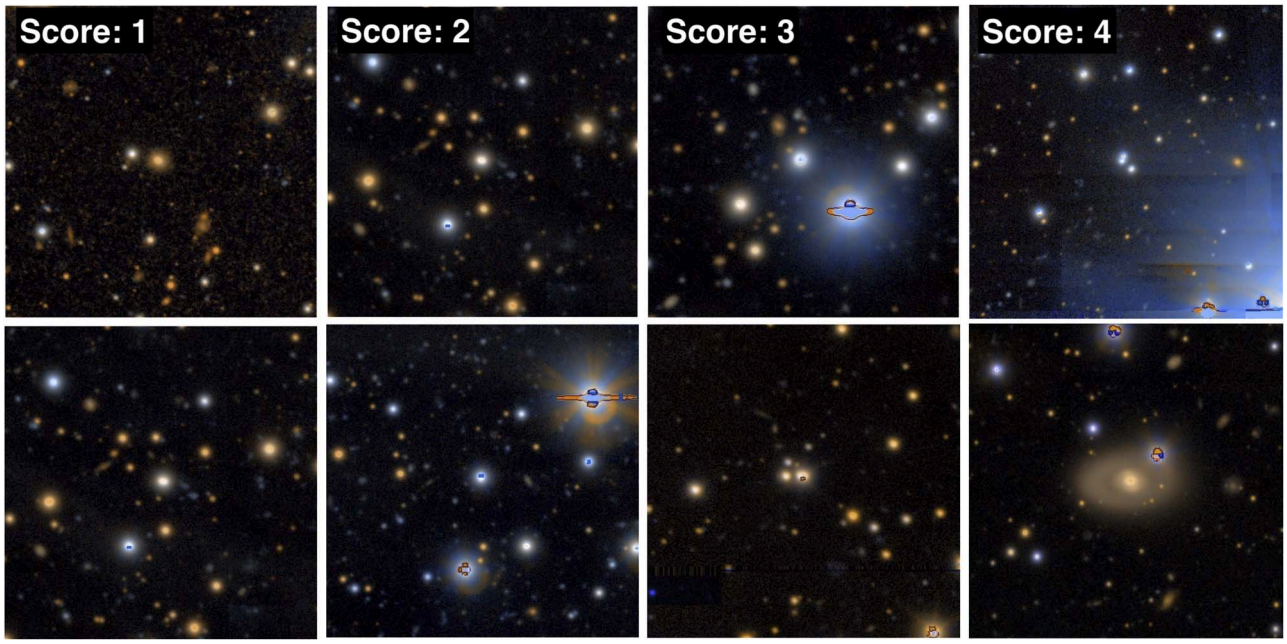

Figure 6. Shown here are $1\farcm2 \times 1\farcm2$ cutouts of PISCeS imaging (Crnojević et al. 2016) for two examples in each category of visual assessment score, as described in the text. Each panel is centered on a UCD candidate identified with the *Gaia* selection criteria. Score 1 objects are the best UCD candidates; Score 2 and 3 are less likely; Score 4 are definite contaminants such as background galaxies (bottom right) or double stars (top right).

typically double stars or background galaxies. We show two examples from each category in Figure 6. A histogram showing the distribution of all candidates we voted on is shown in the top right panel of Figure 7.

3.3. Final Ranking of Star Cluster Candidates

We refine our initial UCD candidate selection where possible by adding in information from (a) the *urz* color selection discussed in Section 2.4 and (b) our visual assessment score from PISCeS imaging discussed above. This additional classification information is not available for all 632 *Gaia* UCD candidates. Of the 346 candidates with PISCeS data, 278 have colors and 68 do not. Of the 286 candidates without PISCeS images, 225 have colors and 61 do not.

Here we discuss our methodology for the final ranking of UCD candidates.

Rank A—Most Probable UCDs. Our Rank A candidates are the most likely UCDs, based on both their colors and visual inspection. This group includes objects with colors that correspond to cluster likelihoods of >0.9 (the inner-most ellipse in Figure 3), and visual assessment scores <2.0 (Figure 6). Figure 7 visually shows their relative ranking in these color and visual assessment categories. Only 11 objects are in this rank, and spectroscopic follow-up of 4 of them (Section 4) has confirmed all as UCDs around Cen A. Their spatial distribution in the halo of Cen A is shown in Figure 8.

Rank B—Good candidate UCDs. Rank B candidates were selected in one of two ways. In the first, the visual or color information strongly suggests that the objects are UCDs (visual assessment score $\leqslant 2.0$ or cluster likelihood $\geqslant 0.9$), but only one of these two pieces of information is available. The other selection method for this rank is candidates with moderately

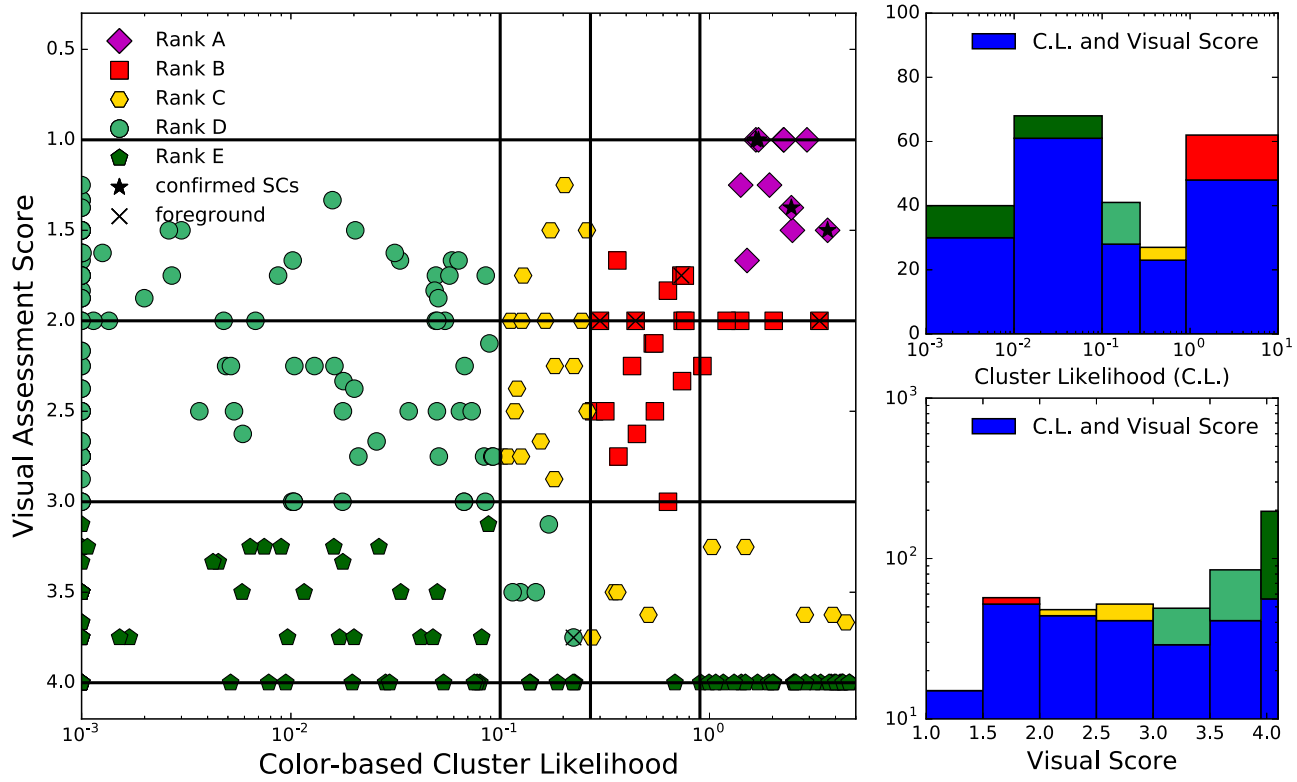

Figure 7. A summary of the ranking of all candidates. The left panel shows targets for which both a color-based likelihood and visual assessment score information are available. Ranks A to E represent most likely to least likely UCDs, with the colors as Rank A (purple); Rank B (red); Rank C (yellow); Rank D (light green); Rank E (dark green). The vertical black lines mark the 0.1, 0.27, and 0.9 relative cluster likelihood levels, which correspond to the three color ellipses (red, orange, and yellow) in Figure 3. Points with a black star in their centers are newly velocity-confirmed UCDs (Section 4), whereas the black crosses mark candidates that are newly confirmed as foreground stars. The histograms on the right show the distribution of all votes and all cluster likelihood values. The blue portion of the histogram marks candidates for which both quantities are available (color and PISCeS imaging), with the added colored bars on top showing the distribution of candidates for which only cluster likelihood or votes are available. The colors of these added bars reflect the associated ranks.

favorable scores for both categories (visual assessment score $\leqslant$3.0 and cluster likelihood $\geqslant$0.27) but that were not high enough for Rank A. There are 42 Rank B candidates. As for Rank A, the spatial distribution of these candidates around Cen A is shown in Figure 8.

Rank C—Candidate UCDs. Rank C includes candidates where the color information and PISCeS imaging data do not suggest a high probability that they are true UCDs, but where this identification is still possible. The details of the classification of objects in this rank can be seen by examining Figure 7. 54 *Gaia* candidates fall into this rank.

Rank D—Candidate UCDs with no additional evidence or conflicting information. Rank D includes the 61 candidates with no PISCeS imaging or color information. It also includes 185 candidates with contradicting information from the votes and probabilities (see Figure 7).

Rank E—Not UCDs. Rank E candidates have colors or imaging that show they are not UCDs. This rank includes all candidates with colors inconsistent with being a UCD and with visual assessment scores $\geqslant$3.0, plus all objects with visual assessment scores of 4 (all team members agreeing that the object is a contaminant). There are 279 *Gaia* candidates which fall into this rank.

A visual summary of these ranks can be found in Figure 7, and complete information for all 632 candidates, including the *Gaia* data, colors, and magnitudes from Taylor et al. (2017) if available, and other classification information, can be found in Table 2. The Taylor colors and magnitudes are all extinction corrected.

3.4. Intrinsic Completeness of Gaia UCD Candidates

One goal of the present work is to provide a complete census of UCDs in the halo of Cen A. Here we analyze the completeness of our sample of new candidates.

In Section 2.1, we showed that all 61 previously known velocity-confirmed UCDs with $g < 19.1$ are detected by *Gaia* and pass our astrometric selection, suggesting a high completeness for this *Gaia*-based UCD search. However, we have visually identified a very extended ($r_h \sim 40$ pc) massive ($\sim 10^6 M_\odot$) star cluster (named "Fluffy"), in the outskirts of Cen A using our PISCeS imaging and with spectroscopic follow-up (see Section 4; D. Crnojevic et al. 2020, in preparation). This object does not appear in the *Gaia* source catalog at all, although its integrated magnitude is theoretically bright enough to make our cuts.

We know from Section 2.2 that we miss 0.5 mag of extended sources in *Gaia*. That Fluffy is not in *Gaia* is thus not surprising as its large size and lower central surface brightness means that the flux enclosed in the *Gaia* aperture may make it too faint to have been cataloged. Diffuse UCDs have been detected in other galaxies, mostly in the Virgo and Fornax Clusters (Brodie et al. 2011; Strader et al. 2012; Forbes et al. 2013; Voggel et al. 2016). They make up a small fraction of the total UCD population, so this source of incompleteness is

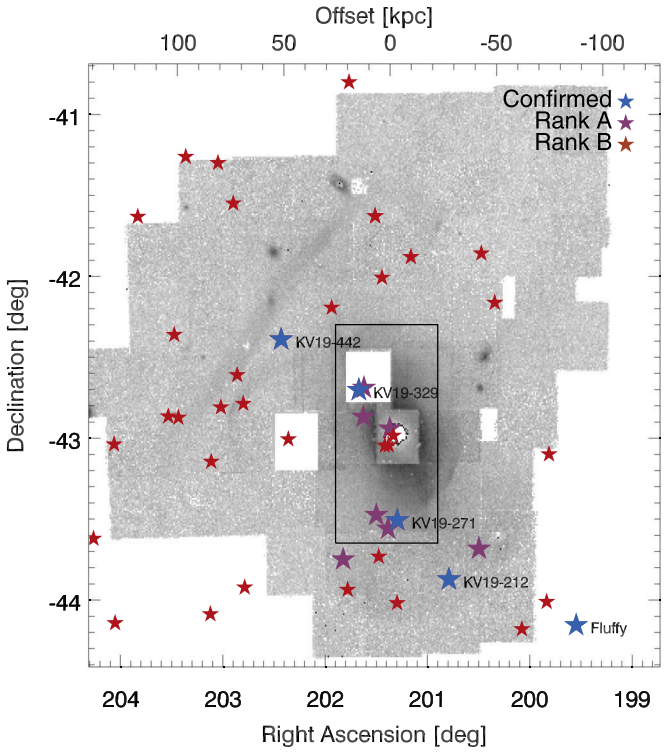

Figure 8. Location of the 11 candidates with Rank A is marked with purple stars, where the five new confirmed UCDs (see Table 3) are shown as blue labeled data points. The Rank B candidates are shown as red stars. The black box marks the area that contains all previously confirmed GCs in Cen A. The background image depicts the stellar halo of Cen A from the PISCeS imaging (Crnojević et al. 2016).

unlikely to be significant, though such objects are strong candidates to be stripped nuclei and hence are worthy of detailed study. Moreover, we have not identified other objects with similar properties in our visual inspection of PISCeS images. In addition, the completeness of *Gaia* sources drops toward fainter magnitudes. For example, the completeness for velocity-confirmed Cen A GCs is ∼90% out to 20′ at $G = 20$ (A. K. Hughes et al. 2020, in preparation). For the sources actually in *Gaia*, nearly all have the astrometric measurements we use to identify candidate UCDs.

Overall our source list appears to be highly complete. Our final candidate list most highly ranks objects where both PISCeS imaging and photometry from Taylor et al. (2017) are available. This is true for only 278 out of 632 (44%) candidates, suggesting that more complete imaging and photometry data could roughly double our sample of Rank A candidates.

4. Follow-up of UCD Candidates

While all of our highly ranked UCD candidates will eventually require spectroscopic follow-up to confirm their nature, here we present the results of our initial efforts to canvass these candidates with spectroscopy.

We obtained spectroscopic follow-up of 14 UCD candidates using the MIKE (Bernstein et al. 2003) on Clay/*Magellan*. We observed three UCD candidates (KV19-442, KV19-329 and KV19-271) on the two nights of 2018 June 16–17 and 10 additional UCD candidates on 2019 April 5–6, as well as the UCD candidate "Fluffy" that was found from PISCeS rather than *Gaia*. All observations consisted of 2 × 1800s exposures.

We reduced the MIKE spectra using the `CarPy` pipeline (Kelson et al. 2000; Kelson 2003). We focus on the spectral order that contains the Ca triplet from 8470 to 8700 Å, which are the deepest and most prominent lines of the spectra. We determined the radial velocities by modeling the spectra of the UCD candidates using a set of 10 template stars observed during the same run with the pPXF package (Cappellari & Emsellem 2004). Here we present only the velocities; a future paper will describe the data and analysis in greater detail, including velocity dispersion measurements and dynamical masses (A. Dumont et al. 2020, in preparation).

The systematic velocity of Cen A is $v_{\rm helio} = 541$ km s^{-1} and the dispersion of its GC system is as high as $\sigma \sim 150$ km s^{-1} (Peng et al. 2004). Stripped nuclei might or might not have a similar velocity dispersion to GCs, but in any case, we can use the GC kinematics as a rough guide to values that should be reasonable for the UCD candidates.

We find that 5 of our 14 candidates have radial velocities that are consistent with being a member of Centaurus A ($v_{\rm helio} = 485$–720 km s^{-1}). The other candidates all have $|v_{\rm helio}| < 50$ km s^{-1} and are thus almost certainly Milky Way foreground stars. A cutout image centered on each confirmed UCD is shown in Figure 9. An example fit zoomed in on the calcium triplet region of the spectra of KV19-442 is shown in Figure 10. The radial velocities of all confirmed UCDs and the foreground objects are listed in Table 3.

The four confirmed *Gaia* UCD candidates (a–d in Table 3) were all Rank A (data points marked with a star in Figure 7) showing that the incidence of true UCDs in this ranking category is high. The remaining nine candidates were of lower ranks (B to D; five points marked with a cross in the left panel of Figure 7, whereas four of them have no visual assessment and are included in the top histogram of Figure 7 with Ranks: twice B, C, and E), consistent with their spectroscopic identification as foreground stars. Additional spectroscopy will be necessary to assess how many UCDs are present in the lower ranks, but it is already clear that both visual classification and colors are useful for effective selection of UCD candidates.

These newly confirmed UCDs are among the most luminous in Cen A. KV19-442 is the 7th and KV19-271 is the 10th most luminous UCD known in Cen A. Fluffy is the most distant known bright GC of Cen A in projection, and the clusters KV19-442 and KV19-212 are also more distant than any previously known GC. These GCs were missed by previous spectroscopic searches due to being located at such large galactocentric radii. This confirmation of UCDs in such a well-studied nearby galaxy shows both the effectiveness and promise of using *Gaia* to find the best UCD candidates for follow-up spectroscopy.

5. Conclusion and Application beyond Cen A

We use the capabilities of *Gaia* to identify new candidate UCDs in the halo of Cen A. Our main results are:

1. We used previously confirmed GCs in Cen A to show that *Gaia* can be used to identify resolved stripped nuclei and luminous star clusters in nearby galaxies.
2. We derived a relation between the sizes of UCDs, *Gaia G* magnitudes, and the *Gaia* astrometric $\rm BR_{excess}$ parameter. This can be used to estimate sizes accurate to ∼30% for extragalactic UCDs with $G < 20$ and sizes ∼0.″1–0.″5.

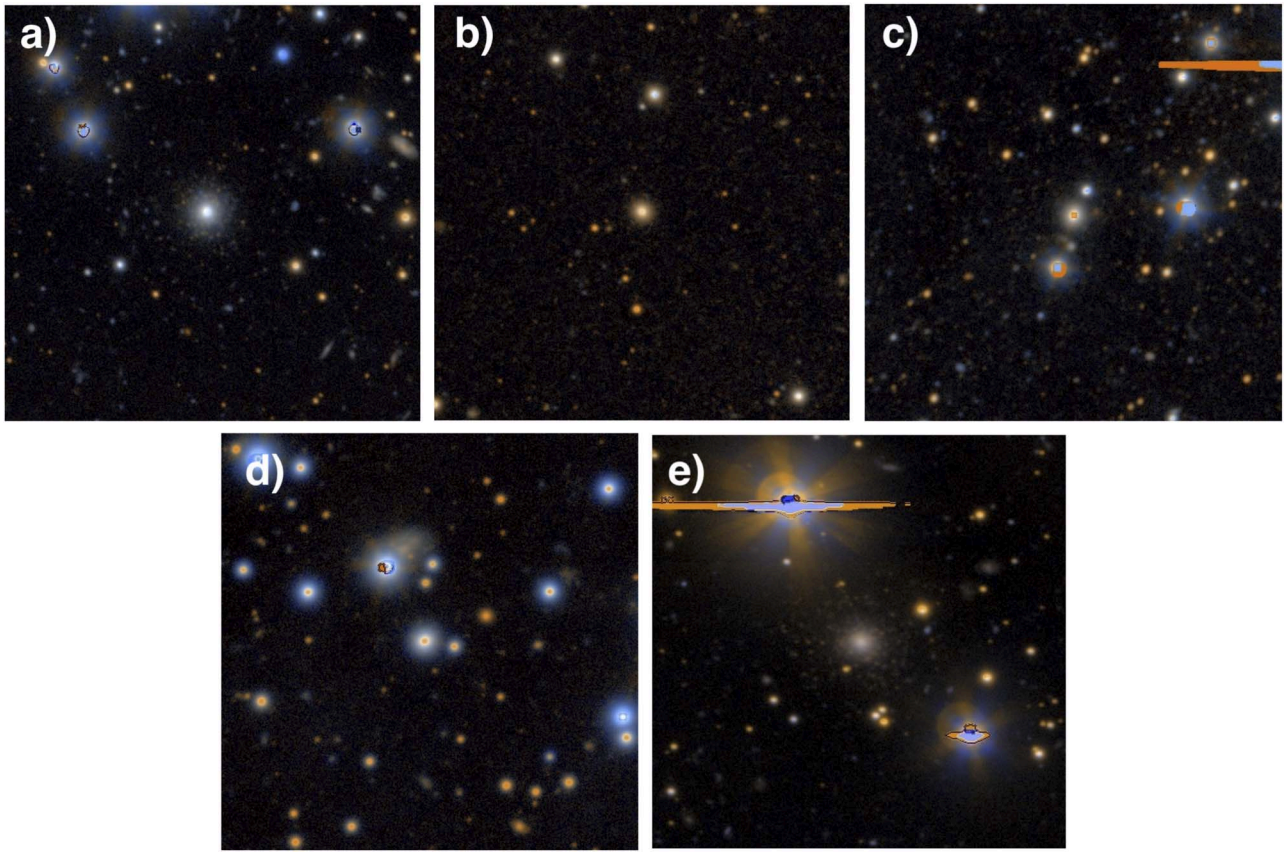

Figure 9. 1.′2 × 1.′2 cutouts show the PISCeS imaging (Crnojević et al. 2016) of the five confirmed UCDs in Centaurus A. The first four panels (a–d) are *Gaia*-selected Rank A UCD candidates, all of which are confirmed; the last panel (e) is the visually selected source "Fluffy."

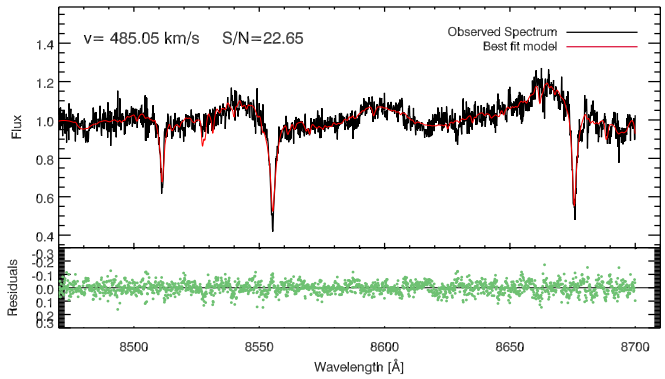

Figure 10. Magellan Inamori Kyocera Echelle spectrograph (MIKE) spectrum of the calcium triplet region of candidate KV19-442 is shown in black. The best fit derived with pPXF is shown in red and the residuals are shown below in green.

We expect this relation can be refined and improved in the future.

3. We apply our new UCD discovery method to obtain a list of *Gaia*-based UCD candidates out to 150 kpc from the center of Cen A. Of these 632 candidates, 91% are at larger radii than any previously velocity-confirmed UCD in Cen A. Down to the magnitude limit of our search ($G < 19$), our tests suggest that our sample is highly complete, except for the rarest, most extended UCDs.
4. Our *Gaia* UCD sample, while mostly complete, is still affected by foreground and background contaminants. Adding in additional imaging and multiband photometry helps substantially in ranking the *Gaia*-based sample.
5. We obtained follow-up spectroscopy of 14 UCD candidates, and confirmed all four of the top-ranked sources observed, including two sources that are now in the top 10 of the most luminous UCDs in Cen A.

For future work, we plan to obtain radial velocities and velocity dispersions for all of the good UCD candidates in this paper. This will enable a large-scale, complete study of stripped nuclei around Cen A, which is an important step in fully reconstructing the assembly history of this keystone galaxy.

5.1. Extension to Other Galaxies

The *Gaia*-based UCD selection introduced here can be used to find UCDs in a much wider range of galaxies, at least in the distance range ∼3–20 Mpc. The lower limit is approximate, based primarily on the fact that we find that most M31 UCDs/GCs (at $D \sim 750$ kpc) are not in *Gaia*, likely because they are too resolved. At the distant end, while a number of Virgo and Fornax UCDs can be found in *Gaia*, the number of sufficiently bright UCDs will decrease substantially at larger distances.

In Figure 11 we show a visual representation of how our UCD selection can be extended to galaxies at different distances and for clusters of different luminosities. The central line is $M_G = -9.7$, equivalent to the selection limit used in the current work to select UCDs with masses above $\sim 10^6\ M_\odot$ (where stripped galaxy nuclei are likely to be present; Voggel et al. 2019). The rightmost line is $M_G = -12.2$, which corresponds to

Table 3
List of MIKE Spectroscopic Targets of *Gaia*-based UCD Candidates

Label	Name	R.A.	Decl.	m_g (mag)	M_g (mag)	Velocity (km s^{-1})	S/N	C.L.	Votes
a	KV19-442	202.432394	−42.391404	17.59	−10.32	485.1 ± 1.2	22.7	1.71	1.0
b	KV19-329	201.672201	−42.703936	17.82	−10.09	627.4 ± 1.6	22.3	1.67	1.0
c	KV19-271	201.296298	−43.509212	17.66	−10.25	548.9 ± 1.7	20.9	3.67	1.5
d	KV19-212	200.790847	−43.874459	17.93	−9.98	535.1 ± 2.4	21.5	2.46	1.4
e	Fluffy	199.545362	−44.157251	18.30	−9.61	719.2 ± 6.4	5.2	⋯	⋯
⋯	KV19-054	199.1021398	−44.5545868	18.04	⋯	0.5 ± 4.3	7.1	5.08	⋯
⋯	KV19-258	201.223936	−44.931836	15.84	⋯	−17.3 ± 6.4	23.0	0.31	⋯
⋯	KV19-397	202.104800	−42.858302	16.26	⋯	−80.8 ± 11.1	16.1	0.22	3.75
⋯	KV19-424	202.321732	−45.212907	15.18	⋯	−81.3 ± 2.0	11.6	10^{-4}	⋯
⋯	KV19-464	202.645456	−44.666926	17.28	⋯	−14.3 ± 32.7	16.1	0.73	1.75
⋯	KV19-492	202.862878	−42.611323	17.89	⋯	−21.9 ± 6.9	8.7	0.44	2.0
⋯	KV19-521	203.050732	−41.300504	17.69	⋯	−95.2 ± 29.1	10.1	2.27	⋯
⋯	KV19-569	203.478425	−42.362577	17.89	⋯	23.6 ± 4.6	10.8	0.30	2.0
⋯	KV19-573	203.537185	−42.866562	18.06	⋯	−19.6 ± 1.7	11.7	3.35	2.0

(This table is available in machine-readable form.)

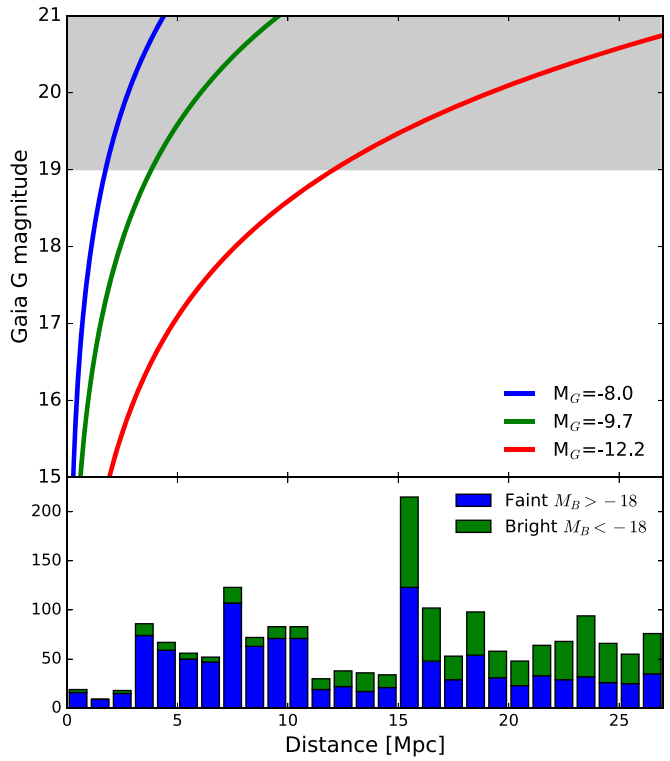

Figure 11. Potential reach of our new *Gaia*-based technique for identifying UCDs. The top plot shows how the apparent magnitude of three different fiducial star clusters evolve as a function of their distance. The horizontal line marks where the availability of the *Gaia* data is essentially complete ($G = 19$), with the gray band above ($19 < G < 21$) marking the region where some useful *Gaia* information is available. The bottom plot is a histogram of the number of galaxies at each distance to show how many bright and fainter galaxies are in principle reachable with this method. For galaxies closer than 11 Mpc we used the sample of Karachentsev et al. (2013) and for more distant galaxies the catalog of Tully (2015).

a mass limit of $\sim 10^7\ M_\odot$, above which a majority of UCDs appear to be stripped nuclei. The leftmost line is $M_G = -8.0$, roughly the peak of the GC luminosity function at $\sim 2 \times 10^5\ M_\odot$. We note that these lines are corrected for the fact that GCs are partially unresolved by *Gaia*—for simplicity we use the same 0.52 magnitude factor derived in Section 2.2; in practice the degree of resolution will likely vary with distance.

We have shown in this paper that at $G < 19$ a nearly complete sample of UCDs can be assembled in Cen A. This same conclusion appears to apply for more distant systems: we find that essentially all of the UCDs with $G \lesssim 19$ in the Virgo UCD catalog of Liu et al. (2015) are in *Gaia*. However, in this same catalog, about half of the UCDs with $19 < G < 21$ are not in *Gaia*. Hence, down to a fainter limit of $G \sim 20$–21 one can construct a reasonable, though not complete, sample of UCDs for more distant galaxies.

The histogram inset to Figure 11 shows the number of galaxies with $M_B < -18$ as a function of distance, where this luminosity limit reflects a guess at those galaxies that could in principle have UCDs detectable with this method. The galaxies are taken from the Karachentsev et al. (2013) and for more distant galaxies from the Tully (2015) catalog. Even if the sample is restricted to brighter galaxies with $M_B < -18$, the number of galaxies for which our method is applicable is appreciable. In the future we plan to carry out a systematic search for UCDs in the halos of all galaxies in the local universe where the method is feasible, though spectroscopic follow-up will likely still be necessary.

The discovery potential (in both distance and UCD mass) will likely grow with the upcoming *Gaia* data release 3, which will provide improved photometry and astrometry. In any case, the present work is already an exciting step toward a better understanding of luminous GCs and stripped nuclei in the local universe.

Work on this project by K.T.V. and A.C.S. was supported by NSF grants AST-1350389 and AST-1813609. Work on this project by D.J.S. and A.H. is supported by NSF grants AST-1821967 and 1813708. J.S. is supported by NSF grant AST-1812856 and the Packard Foundation. Research by D.C. is supported by NSF grant AST-1814208, and by NASA through grants number HST-GO-15426.007-A and HST-GO-15332.004-A from the Space Telescope Science Institute, which is operated by AURA, Inc., under NASA contract NAS

5-26555. This research uses services or data provided by the NOAO Data Lab. NOAO is operated by the Association of Universities for Research in Astronomy (AURA), Inc. under a cooperative agreement with the National Science Foundation.

Software: This research made use of Astropy,[8] a community-developed core Python package for Astronomy (Astropy Collaboration et al. 2013; Price-Whelan et al. 2018). This research has made use of NASA's Astrophysics Data System, the Scikit-learn (Pedregosa et al. 2011) code, the SciPy (Virtanen et al. 2020) package and NumPy (Van Der Walt et al. 2011). We also gratefully acknowledge the use of the Carnegie Python Distribution (CarPy) that provided the MIKE data reduction pipeline (Kelson et al. 2000; Kelson 2003).

Facilities: Magellan:Clay (Megacam), *Gaia*.

Appendix
Literature GCs Used for Completeness Assessment

A complete list of the 57 literature GCs used in this comparison can be found in Table A1.

Table A1
List of the 57 Previously Confirmed UCDs that Were Used to Assess Completeness in Figure 1

Taylor 2017 Name	R.A. (°)	Decl. (°)	Gaia *G*	AEN	BR_{excess}	Taylor 2017 *g*' (mag)
T17-1002	200.909654	−42.773053	18.87	9.13	2.40	18.09
T17-1008	200.926390	−43.160493	19.54	15.29	2.82	18.76
T17-1020	200.956660	−43.242243	19.09	6.73	2.10	18.62
T17-1050	200.994829	−43.026381	19.31	10.01	2.75	18.70
T17-1110	201.075206	−42.816957	18.91	6.53	2.39	18.16
T17-1188	201.153561	−43.321188	19.42	9.03	2.31	18.73
T17-1197	201.162357	−43.335133	18.72	3.86	2.09	18.38
T17-1202	201.168229	−43.301482	18.46	6.36	2.46	17.93
T17-1203	201.168337	−43.584709	19.44	7.22	2.50	18.73
T17-1207	201.170003	−42.683779	18.69	2.71	1.91	18.43
T17-1232	201.194548	−43.021799	19.43	8.58	3.10	18.74
T17-1243	201.200123	−43.137294	18.82	4.90	2.56	18.30
T17-1260	201.211852	−43.023042	19.13	5.19	2.98	18.77
T17-1264	201.214461	−43.203099	18.86	4.47	2.58	18.24
T17-1284	201.226439	−42.890201	17.39	3.29	2.03	17.10
T17-1287	201.227938	−43.022712	18.20	5.12	2.74	17.78
T17-1313	201.239246	−43.018940	18.47	4.11	2.49	18.27
T17-1314	201.239568	−42.989816	19.13	7.50	3.06	18.58
T17-1322	201.242499	−42.936123	17.98	3.03	2.47	17.60
T17-1347	201.254756	−42.947666	18.94	4.20	2.42	18.62
T17-1358	201.257506	−43.157080	18.58	10.72	3.02	17.82
T17-1375	201.263984	−42.846132	18.64	3.58	2.33	18.32
T17-1386	201.269934	−43.160808	18.99	9.41	2.77	18.43
T17-1388	201.270881	−42.954239	17.53	3.96	2.15	17.27
T17-1395	201.273696	−43.175240	18.24	3.95	2.52	17.85
T17-1400	201.275932	−43.253251	19.12	8.39	2.78	18.52
T17-1430	201.292744	−42.892504	18.16	4.91	2.65	17.65
T17-1432	201.293668	−42.747977	18.30	5.61	2.37	17.72
T17-1447	201.300810	−43.276086	19.30	6.39	2.29	18.72
T17-1455	201.303631	−43.133121	18.27	3.41	2.16	18.06
T17-1486	201.317717	−42.848126	18.91	8.17	2.58	18.31
T17-1596	201.376623	−43.197138	19.05	13.03	3.02	18.46
T17-1611	201.382221	−43.322982	19.08	8.44	2.36	18.48
T17-1616	201.386606	−43.117305	18.95	4.60	2.66	18.63
T17-1639	201.395821	−42.601374	18.90	5.17	2.35	18.41
T17-1664	201.407701	−42.941120	18.87	3.08	2.85	18.76
T17-1682	201.415494	−42.933094	18.04	8.38	2.86	17.48
T17-1688	201.419139	−43.353852	18.68	4.35	2.36	18.26
T17-1719	201.430767	−43.123036	18.60	9.20	2.93	18.01
T17-1773	201.457002	−42.913691	18.31	6.30	2.72	17.83
T17-1780	201.458071	−42.869243	19.07	5.22	2.69	18.58
T17-1805	201.469692	−43.096254	18.20	4.98	2.51	17.74
T17-1814	201.473123	−42.985426	18.37	4.49	2.64	18.01
T17-1887	201.505241	−43.570995	18.83	5.73	2.46	18.26
T17-1899	201.511786	−42.949167	18.81	4.74	3.05	18.46
T17-1920	201.522473	−42.942327	17.56	5.45	2.54	17.02
T17-1940	201.532144	−42.866721	18.67	4.95	2.33	18.26
T17-1957	201.544021	−42.895178	18.53	3.20	2.15	18.37

[8] http://www.astropy.org

Table A1
(Continued)

Taylor 2017 Name	R.A. (°)	Decl. (°)	Gaia G	AEN	BR_{excess}	Taylor 2017 g' (mag)
T17-1973	201.563543	−42.808167	18.43	5.518	2.57	18.18
T17-1974	201.566080	−42.916914	18.12	1.76	1.78	17.89
T17-1989	201.581834	−43.055186	19.15	6.43	2.63	18.65
T17-2013	201.599019	−42.900293	18.69	5.35	2.27	18.37
T17-2018	201.600676	−42.783526	18.84	6.78	2.37	18.41
T17-2064	201.660367	−42.762706	19.08	8.37	2.61	18.50
T17-2091	201.689029	−43.442810	19.06	4.47	2.13	18.59
T17-2107	201.724630	−43.321591	18.50	3.90	2.02	18.19
T17-2133	201.764179	−42.454757	18.66	3.99	2.27	18.27

Note. The Taylor 2017 g' magnitudes are from their Table 2 and are already extinction corrected.

(This table is available in machine-readable form.)

ORCID iDs

Karina T. Voggel https://orcid.org/0000-0001-6215-0950
Anil C. Seth https://orcid.org/0000-0003-0248-5470
David J. Sand https://orcid.org/0000-0003-4102-380X
Jay Strader https://orcid.org/0000-0002-1468-9668
Denija Crnojevic https://orcid.org/0000-0002-1763-4128
Nelson Caldwell https://orcid.org/0000-0003-2352-3202

References

Afanasiev, A. V., Chilingarian, I. V., Mieske, S., et al. 2018, MNRAS, 477, 4856
Ahn, C. P., Seth, A. C., Cappellari, M., et al. 2018, ApJ, 858, 102
Ahn, C. P., Seth, A. C., den Brok, M., et al. 2017, ApJ, 839, 72
Astropy Collaboration, Robitaille, T. P., Tollerud, E. J., et al. 2013, A&A, 558, A33
Beasley, M. A., Bridges, T., Peng, E., et al. 2008, MNRAS, 386, 1443
Bekki, K., Couch, W. J., & Drinkwater, M. J. 2001, ApJL, 552, L105
Bekki, K., Couch, W. J., Drinkwater, M. J., & Shioya, Y. 2003, MNRAS, 344, 399
Bekki, K., & Freeman, K. C. 2003, MNRAS, 346, L11
Bernstein, R., Shectman, S. A., Aunnels, S. A., Mochnacki, S., & Athey, A. E. 2003, Proc. SPIE, 4841, 1694
Brodie, J. P., Romanowsky, A. J., Strader, J., & Forbes, D. A. 2011, AJ, 142, 199
Cappellari, M., & Emsellem, E. 2004, PASP, 116, 138
Crnojević, D., Sand, D. J., Bennet, P., et al. 2019, ApJ, 872, 80
Crnojević, D., Sand, D. J., Caldwell, N., et al. 2014, ApJL, 795, L35
Crnojević, D., Sand, D. J., Spekkens, K., et al. 2016, ApJ, 823, 19
Da Rocha, C., Mieske, S., Georgiev, I. Y., et al. 2011, A&A, 525, A86
den Brok, M., Peletier, R. F., Seth, A., et al. 2014, MNRAS, 445, 2385
Evans, D. W., Riello, M., De Angeli, F., et al. 2018, A&A, 616, A4
Forbes, D. A., Pota, V., Usher, C., et al. 2013, MNRAS, 435, L6
Gaia Collaboration, Brown, A. G. A., Vallenari, A., et al. 2018, A&A, 616, A1
Georgiev, I. Y., & Böker, T. 2014, MNRAS, 441, 3570
Georgiev, I. Y., Böker, T., Leigh, N., Lützgendorf, N., & Neumayer, N. 2016, MNRAS, 457, 2122
Gómez, M., Geisler, D., Harris, W. E., et al. 2006, A&A, 447, 877
Harris, G. L. H., Geisler, D., Harris, H. C., & Hesser, J. E. 1992, AJ, 104, 613
Harris, G. L. H., Gómez, M., Harris, W. E., et al. 2012, AJ, 143, 84
Harris, G. L. H., Rejkuba, M., & Harris, W. E. 2010, PASA, 27, 457
Harris, W. E., Harris, G. L. H., Barmby, P., McLaughlin, D. E., & Forbes, D. A. 2006, AJ, 132, 2187
Harris, W. E., Harris, G. L. H., Holland, S. T., & McLaughlin, D. E. 2002, AJ, 124, 1435
Hilker, M. 2006, arXiv:astro-ph/0605447
Jordi, C., Gebran, M., Carrasco, J. M., et al. 2010, A&A, 523, A48
Karachentsev, I. D., Makarov, D. I., & Kaisina, E. I. 2013, AJ, 145, 101
Kelson, D. D. 2003, PASP, 115, 688
Kelson, D. D., Illingworth, G. D., van Dokkum, P. G., & Franx, M. 2000, ApJ, 531, 159
Lindegren, L., Hernández, J., Bombrun, A., et al. 2018, A&A, 616, A2
Liu, C., Peng, E. W., Côté, P., et al. 2015, ApJ, 812, 34
Martini, P., & Ho, L. C. 2004, ApJ, 610, 233
Muñoz, R. P., Puzia, T. H., Lançon, A., et al. 2014, ApJS, 210, 4
Norris, M. A., Escudero, C. G., Faifer, F. R., et al. 2015, MNRAS, 451, 3615
Norris, M. A., & Kannappan, S. J. 2011, MNRAS, 414, 739
Norris, M. A., Kannappan, S. J., Forbes, D. A., et al. 2014, MNRAS, 443, 1151
Pedregosa, F., Varoquaux, G., Gramfort, A., et al. 2011, J. Mach. Learn. Res., 12, 2825
Peng, E. W., Ford, H. C., & Freeman, K. C. 2004, ApJS, 150, 367
Pfeffer, J., & Baumgardt, H. 2013, MNRAS, 433, 1997
Pfeffer, J., Hilker, M., Baumgardt, H., & Griffen, B. F. 2016, MNRAS, 458, 2492
Portegies Zwart, S. F., & McMillan, S. L. W. 2002, ApJ, 576, 899
Price-Whelan, A. M., Sipócz, B. M., Günther, H. M., et al. 2018, AJ, 156, 123
Rejkuba, M., Dubath, P., Minniti, D., & Meylan, G. 2007, A&A, 469, 147
Sánchez-Janssen, R., Côté, P., Ferrarese, L., et al. 2019, ApJ, 878, 18
Schlafly, E. F., & Finkbeiner, D. P. 2011, ApJ, 737, 103
Seth, A. C., van den Bosch, R., Mieske, S., et al. 2014, Natur, 513, 398
Strader, J., Caldwell, N., & Seth, A. C. 2011, AJ, 142, 8
Strader, J., Fabbiano, G., Luo, B., et al. 2012, ApJ, 760, 87
Taylor, M. A., Muñoz, R. P., Puzia, T. H., et al. 2016, arXiv:1608.07285
Taylor, M. A., Puzia, T. H., Harris, G. L., et al. 2010, ApJ, 712, 1191
Taylor, M. A., Puzia, T. H., Muñoz, R. P., et al. 2017, MNRAS, 469, 3444
Tully, R. B. 2015, AJ, 149, 54
Van Der Walt, S., Colbert, S. C., & Varoquaux, G. 2011, CSE, 13, 22
Virtanen, P., Gommers, R., Oliphant, T. E., et al. 2020, Nat. Methods, 17, 261
Voggel, K., Hilker, M., & Richtler, T. 2016, A&A, 586, A102
Voggel, K. T., Seth, A. C., Baumgardt, H., et al. 2019, ApJ, 871, 159
Wetzel, A. R., Hopkins, P. F., Kim, J.-h., et al. 2016, ApJL, 827, L23
Woodley, K. A., Gómez, M., Harris, W. E., Geisler, D., & Harris, G. L. H. 2010a, AJ, 139, 1871
Woodley, K. A., Harris, W. E., Beasley, M. A., et al. 2007, AJ, 134, 494
Woodley, K. A., Harris, W. E., & Harris, G. L. H. 2005, AJ, 129, 2654
Woodley, K. A., Harris, W. E., Puzia, T. H., et al. 2010b, ApJ, 708, 1335